Dielectric Characterization of *Ex Vivo* Ovine and Human Adrenal Glands for Microwave Thermal Ablation Applications

Anna Bottiglieri, Atif Shahzad, Padraig Donlon, Michael Conall Dennedy, Aoife Lowery, Martin O'Halloran, *Member, IEEE*, and Laura Farina, *Member, IEEE*

***Abstract*—Historically, adrenal glands diseases causing hypertension, such as Primary Aldosteronism (PA), have been treated through pharmacotherapy or surgical resection. Given the shortcomings of the available treatment options, the interest in alternative and less invasive treatment modalities such as microwave ablation (MWA), has increased. In order to develop and optimize this novel electromagnetic-based therapy, an accurate knowledge of the dielectric properties of human adrenal glands, as well as preclinical animal models, is crucial. In particular, ovine models represent a feasible animal model to test the safety and performances of MWA. In this study, the dielectric properties of ovine adrenal glands and of normal and diseased human adrenal glands are characterized *ex vivo* in the microwave frequency range. The dielectric properties of the two functional tissues (cortex and medulla) composing ovine adrenal glands are measured using the open-ended coaxial probe technique and represented with a two pole Cole-Cole model in the frequency range from 0.5 GHz to 8 GHz. This paper presents the first dielectric data of normal and diseased human adrenal tissues, including a functioning adenoma responsible for PA and it compares the human data with data from the animal model.**

***Index Terms*—Dielectric properties, microwave thermal ablation, adrenal gland, open-ended coaxial probe, Cole-Cole model.**

Manuscript received September 24, 2020; revised December 11, 2020 and January 8, 2021; accepted January 11, 2021. Date of publication January 15, 2021; date of current version August 21, 2021. This work was supported in part by the Science Foundation Ireland (SFI) and is co-funded under the European Regional Development Fund under Grant 13/RC/2073 and in part by the European Union Horizon 2020 Research and Innovation Programme under the Marie Skłodowska-Curie Grant 713690, in part by the European Research Council under the European Union's Horizon 2020 Programme (H2020)/ERC under Grant 637780, in part by Irish Research Council Postdoctoral Fellowship under Grant GOIPD/2018/644, in part by the Science Foundation Ireland under Grant 18/USNIH/010, and in part by the framework of COST Action CA17115 "MyWAVE". *(Corresponding author: Laura Farina.)*

Anna Bottiglieri is with the Translational Medical Device Lab, National University of Ireland Galway, Galway, Ireland, and also with the Deptartment of Electrical and Electronic Engineering, National University of Ireland Galway, Galway, Ireland (e-mail: a.bottiglieri1@nuigalway.ie).

Atif Shahzad and Martin O'Halloran are with the Translational Medical Device Lab, National University of Ireland Galway, Galway, Ireland (e-mail: atif.shahzad@ nuigalway.ie; martin.ohalloran@ nuigalway.ie).

Padraig Donlon and Michael Conall Dennedy are with the Discipline of Pharmacology and Therapeutics, School of Medicine, National University of Ireland Galway, Galway, Ireland (e-mail: p.donlon2@nuigalway.ie; michael.dennedy@nuigalway.ie).

Aoife Lowery is with the Discipline of Surgery, Lambe Institute for Translational Research, National University of Ireland Galway, Galway, Ireland (e-mail: aoife.lowery@nuigalway.ie).

Laura Farina is with the Translational Medical Device Lab, National University of Ireland Galway, Galway, Ireland, and also with CÚRAM, SFI Research Centre for Medical Devices, Galway, Ireland (e-mail: laura.farina@nuigalway.ie).

Digital Object Identifier 10.1109/JERM.2021.3052108

I. Introduction

THE adrenal glands are paired organs located on the top of the kidneys, each one surrounded by a fat capsule. The gland is characterized by two functional tissues: the inner tissue named medulla and the external tissue named cortex. The cortex is responsible for the regulation of blood pressure, through the release of the aldosterone hormone [1].

Within the different types of endocrine tumours that can affect adrenal glands, adreno-cortical adenoma is the most common adrenal tumour [2], [3]. In the cases of adreno-cortical adenomas inducing unregulated production of the aldosterone hormone and the consequent increase of the blood pressure, the pathological state is called Primary Aldosteronism (PA) [4], [5]. The current curative approach to unilateral PA is surgical resection of the gland. Bilateral disease is currently managed, but not definitevely treated, through pharmacotherapy. Hence, a less invasive and more effective treatment appears a clear requirement, to completely cure the condition with minimal side effects [6]–[8]. Thermal ablation techniques represent an effective potential alternative in the context of these cancerous lesions treatment [9], [10]. In particular, microwave ablation (MWA) has been recently investigated as an alternative approach for the treatment of adrenal diseases [11], [12]. The objective of the thermal ablation techniques is to induce coagulation necrosis of the cancerous cells by increasing the temperature above 50–60 $^{\circ}$C in the target tissue [9], [13], [14]. The increase of temperature is achieved through the interaction between the target tissue and the electromagnetic (EM) field excited by an interstitial antenna at 915 MHz, 2.45 GHz or 5.8 GHz [15], [16].

The interactions of the EM field with the surrounding tissues are governed by the relative permittivity and the effective conductivity of the tissues. Therefore, a comprehensive knowledge of the dielectric properties of the biological tissues enables accurate simulations of the antenna performances, the optimization of the antenna geometry and the power delivery settings facilitating accurate modelling of new medical devices as well as human safety studies [17]–[20].

Although a large number of experimental studies was conducted acquiring the dielectric properties of healthy and diseased

tissues [21]–[26], the literature reports only a limited number of data on the dielectric properties of adrenal glands [27], [28]. In [27], the dielectric properties of the outer layer of the gland (the cortex) are measured in *in vivo* porcine models; while in [28] the dielectric properties of *ex vivo* bovine adrenal glands are measured distinguishing between the cortex and the medulla.

In this study, measurements of the dielectric properties of freshly excised ovine tissues (eight samples, N = 48) were conducted, distinguishing between the cortex and the medulla. The data are reported together with the optimized parameters of the two pole Cole-Cole model. The ovine model has been chosen for this study since it is a good candidate for pre-clinical studies for a comprehensive experimental investigation of novel ablative approaches [29], [30]; ovine models are indeed currently adopted [31]–[33].

Moreover, in this study, for the first time, the dielectric properties of normal and diseased (i.e. parganglioma, pheochromocytoma, non-functioning nodule and aldosterone-producing adenoma) *ex vivo* human adrenal tissues (six samples, N = 39) are presented. The remainder of the paper is organized as follows: in Section II the materials and the measurement method of the dielectric properties with the related uncertainty values are described. In Section III, the results of the measurements of dielectric properties related to the *ex vivo* ovine and *ex vivo* human adrenal glands are reported and discussed. In Section IV, the conclusions are presented.

II. Methods

A. Source of Tissue

Eight adrenal glands (N = 8) of 16.0 ± 1.0 mm (length), 8.0 ± 1.0 mm (width), 6.0 ± 1 mm (thickness) with medulla sizes ranging between 3–4 mm in width and 8–9 mm in length, were obtained from the local slaughterhouse immediately after their excision from eight different animals and transported to our laboratories in sealed containers; the samples arrived in our laboratories within one hour from excision. The glands remained embedded within their fat capsule to prevent the dehydration of the tissues. Once in the laboratory, the adrenal glands were separated from their surrounding structures, including the kidney, and the fat capsule was kept in place.

The protocol for measuring dielectric properties of *ex vivo* human adrenal glands, was approved by the Galway University Hospitals Research Ethics Committee. Six patients (N = 6) with diagnosed adrenal abnormalities and scheduled to undergo unilateral adrenalectomy were included in the study. The examined human adrenal samples varied between 9 mm to 70 mm in maximum dimension. The types of adrenal abnormalities include: paraganglioma (n = 1), pheochromocytoma (n = 3), non-functioning nodule (n = 1) and aldosterone-producing adenoma (n = 1) which is responsible for PA condition. In two of six samples, measurements of the normal healthy tissue were also acquired: on the normal tissue adjacent to the pheochromocytoma and on the normal tissue surrounding the non-functioning nodule.

In the cases where either the histology analysis or the gross description of the removed gland was not provided by the pathologist, the sample was excluded from the study.

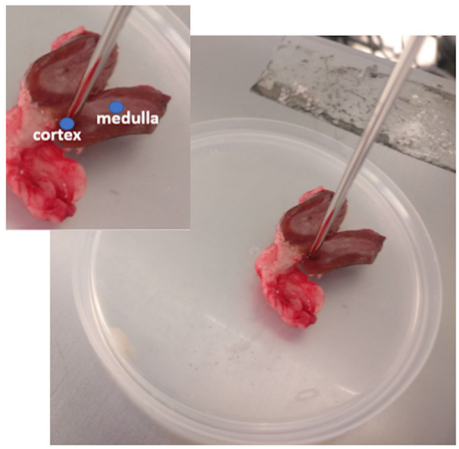

Fig. 1. Example of *ex vivo* ovine adrenal gland in contact with the open-ended coaxial probe. The measurement points are marked and labeled.

B. Dielectric Properties Acquisition

The measurements of the dielectric properties were performed using a slim form open-ended coaxial probe (Keysight 85070E, Santa Rosa, CA, US). Extensive prior studies demonstrated the reliable performances of the slim form coaxial probe. In this study, the 2.2 mm diameter probe allowed consistent contact with the tissue sample, resulting in robust performances. The sensing depth of the probe is within 1 mm [34], while the sensing radius is 1 mm beside the diamater of the probe [35]. For each measurement, the tip of the probe was placed in contact with the tissue under test, as shown in Fig. 1. A vector network analyser (Keysight VNA E5063A, Santa Rosa, CA, US) was used to record the reflection coefficient at the calibration plane of the probe. The data were recorded at 101 linearly spaced frequency points over a frequency range from 0.5 GHz to 8 GHz. The conversion from the complex reflection coefficient into the real part ($\varepsilon'(\omega)$) and imaginary part ($\varepsilon''(\omega)$) of the complex permittivity ($\varepsilon^*(\omega)$) is automatically executed by the Keysight software (Keysight N1500A, Santa Rosa, CA, US) [36]. A lift table was used to position the tissue sample in contact with the probe, connected directly to the port of the VNA, in order to limit the effect of any cable movement in the dielectric data and to enhance the contact between the probe and the sample [36]. The measurement pressure was adjusted to ensure repeatable measurements on the same measurement location following the protocol adopted in [36]. The temperature of each sample was costantly monitored using an infrared termometer in order to maintain the integrity of the tissue.

The ovine samples were sectioned to provide access to both the cortex and the medulla layers: one measurement location was identified for each layer and three measuraments were performed in the same location, for a total of 48 measurements and 16 measurements points (8 for the cortex and 8 for the medulla). On average the temperature of the *ex vivo* ovine samples was 22.2 ± 1.5 °C. The probe was cleaned with alcohol wipe prior to every measurement.

Measurements on *ex vivo* human adrenal glands were performed on each tissue type indicated by the surgeon in the operating room. Approximately 30 min after the resection,

the sample was transported to the pathology room where the measurements were performed following the same experimental protocol adopted in the animal study. The temperature of the samples varied between 20 °C and 23 °C. The probe was placed at up to five different locations of a given tissue type, depending on the size of the sample, and up to three frequency sweeps were performed at each location. The measurement locations were marked for the following histology analysis. The type of tissue underlying the measurement locations was then univocally identified by the histological analysis; where a univocal identification was not possible the measurement location was discarded. Accordingly, only 39 measurements obtained from 6 different samples were included in this study out of 147 collected on 16 samples."

C. Calibration and Validation

Calibration was performed before each measurement of biological tissue, in order to visualize and compensate the main sources of error; each measurement session did not exceed a 2 h duration [36]. Measurements on three standard loads were peformed: open circuit, short circuit and deionized (DI) water [36]. The mean values of temperature of the DI water used for the calibration both for *ex vivo* animal study and *ex vivo* human study were 23.5 ± 0.4 °C and 22.1 ± 0.2 °C, respectively. The quality of the calibration was validated with measurements on reference liquids. Measurements on 0.1 M NaCl solution were executed immediately following the calibration and compared with literature data, before acquiring the set of dielectric data on the biological tissue, as in [36], [37]. A second validation was conducted also right after the measurements on the biological tissue. A total of eight and fourteen measurements on 0.1 M NaCl solutions were performed during the study for the dielectric characterization of *ex vivo* ovine adrenal glands and *ex vivo* human adrenal tissues, respectively. The mean values of temperature of the 0.1 M NaCl solution used for the validation both for *ex vivo* animal study and *ex vivo* human study were 23.4 ± 0.2 °C and 22.3 ± 0.2 °C, respectively.

D. Measurement uncertainty

Three main uncertainty sources were identified and calculated within the measurements performed on 0.1 M NaCl solution, using the standard analysis explained in [38]. The components of uncertainty related to the repeatibility, accuracy and drift error of the measurement system were estimated for each frequency point and averaged over the frequency band of the measurement.

The uncertainty related to the repeatability provides a measure of the random errors affecting the measurement process. The repeatability is expressed as the standard deviation of the data that are repeatedly acquired under the same measurement conditions. The uncertainty component linked to the accuracy of the measurements is the averaged percentage difference between the acquired data and the reference model; in this study the reference model is reported in [37]. Finally, the uncertainty related to the drift was considered evaluating the variability in the dielectric values of deionized water across different calibrations.

TABLE I
CALCULATION OF UNCERTAINTY COMPONENTS, COMBINED UNCERTAINTY AND EXPANDED UNCERTAINTY FOR MEASURED PERMITTIVITY AND CONDUCTIVITY OF 0.1 M NACL, IN THE FREQUENCY RANGE 0.5–8 GHZ. THE UNCERTAINTY ELEMENTS ARE RELATED TO THE VALIDATION PROCESSES PERFORMED PRIOR TO THE DIELECTRIC ANALYSIS ON *EX VIVO* OVINE ADRENAL TISSUES

	Uncertainty component (%) a	Probability distribution	Divisor b	Standard Uncertainty (%) $u_i = \frac{a}{b}$
Permittivity				
Repeatability	1.6	N	1	1.6
Accuracy	2.4	R	$\sqrt{3}$	1.4
Drift	0.05	R	$\sqrt{3}$	0.03
Combined Uncertainty (u_c)	2.2	$u_c = \sqrt{\sum u_i^2}$		
Expanded Uncertainty (u_e, $k = 2$)	4.4	$u_e = ku_c$		
Conductivity				
Repeatability	0.9	N	1	0.9
Accuracy	2.2	R	$\sqrt{3}$	1.3
Drift	0.1	R	$\sqrt{3}$	0.06
Combined Uncertainty (u_c)	1.6	$u_c = \sqrt{\sum u_i^2}$		
Expanded Uncertainty (u_e, $k = 2$)	3.2	$u_e = ku_c$		

N = normal distribution, R = rectangular distribution

In this work, the uncertainty arising from the cable movement was not considered since the probe remains fixed to the port of the VNA during the measurements. Each uncertainty component (u_i) was used to calculate the combined uncertainty (u_c), then the expanded uncertainty (u_e) was calculated considering a 95% confidence interval, according to the guidelines of the National Institute of Standard and Technology (NIST) [39]. The values of the expanded uncertainty related to the *ex vivo* ovine study are 4.4% for the relative permittivity and 3.2% for the conductivity. In Table I, each uncertainty component, the combined and the expanded uncertainties are listed both for the relative permittivity and effective conductivity.

The calculation of each uncertainty component related to the *ex vivo* human study was performed following the same method adopted in the animal study. The values of the expanded uncertainty related to the *ex vivo* human study are 1.4% for the relative permittivity and 4.0% for the effective conductivity. In Table II the values of each uncertainty component are reported. These data are affected by the different number of measurements when compared with animal data, and by the more controlled environmental parameters of the pathology room.

E. Data analysis

The dielectric spectrum of the tissues presented in this study which spans from 0.5 GHz to 8 GHz, contains two main dispersions (the end tail of β dispersion and part of the γ dispersion)

TABLE II
CALCULATION OF UNCERTAINTY COMPONENTS, COMBINED UNCERTAINTY AND EXPANDED UNCERTAINTY FOR MEASURED PERMITTIVITY AND CONDUCTIVITY OF 0.1 M NACL, IN THE FREQUENCY RANGE 0.5–8 GHZ. THE UNCERTAINTY ELEMENTS ARE RELATED TO THE VALIDATION PROCESSES PERFORMED PRIOR TO THE DIELECTRIC ANALYSIS ON *EX VIVO* HUMAN ADRENAL TISSUES

	Uncertainty component (%) a	Probability distribution	Divisor b	Standard Uncertainty (%) $u_i = \frac{a}{b}$
Permittivity				
Repeatability	0.5	N	1	0.5
Accuracy	0.7	R	$\sqrt{3}$	0.4
Drift	0.04	R	$\sqrt{3}$	0.02
Combined Uncertainty (u_c)	0.7	$u_c = \sqrt{\sum u_i^2}$		
Expanded Uncertainty (u_e, $k = 2$)	1.4	$u_e = ku_c$		
Conductivity				
Repeatability	0.7	N	1	0.7
Accuracy	3.1	R	$\sqrt{3}$	1.8
Drift	0.05	R	$\sqrt{3}$	0.03
Combined Uncertainty (u_c)	2.0	$u_c = \sqrt{\sum u_i^2}$		
Expanded Uncertainty (u_e, $k = 2$)	4.0	$u_e = ku_c$		

N = normal distribution, R = rectangular distribution

TABLE III
PARAMETERS OF THE TWO POLE COLE-COLE MODEL FITTED (5,000 ITERATIONS) TO THE MEASURED ADRENAL DATA (CORTEX AND MEDULLA), IN THE FREQUENCY RANGE 0.5–8 GHZ

	This study		Shahzad et al., 2017	
Parameter	Cortex	Medulla	Cortex	Medulla
ε_∞	1.0	1.8	3.57	3.88
$\Delta\varepsilon_1$	45.3	51.1	47.08	52.95
τ_1	6.4 ps	7.1 ps	8.33 ps	7.01 ps
α_1	0.1	0.1	0.16	0.17
$\Delta\varepsilon_2$	54.6	60.5	52.31	62.05
τ_2	1.7 ns	1.3 ns	1.69 ns	4.28 ns
α_2	0.1	0.1	0.03	0.14
σ_s	0.4	0.4	0.46	0.62

[24]. To obtain the analytical expression of the dielectric spectrum of the *ex vivo* ovine data, a two pole Cole-Cole model was used for the representation of the frequency dependent experimental data:

$$\varepsilon^*(\omega) = \varepsilon_\infty + \frac{\Delta\varepsilon_1}{1 + (j\omega\tau_1)^{(1-\alpha_1)}} + \frac{\Delta\varepsilon_2}{1 + (j\omega\tau_2)^{(1-\alpha_2)}} + \frac{\sigma_s}{j\omega\varepsilon_0} \quad (1)$$

where ε_∞ is the permittivity at infinite frequencies, $\Delta\varepsilon_1$ and $\Delta\varepsilon_2$ are the changes in the permittivity for the first and second pole, τ_1 and τ_2 are the relaxation times for the first and second dispersion, α_1 and α_2 are empirical parameters that account for the distribution of the relaxation time and σ_s (S/m) is the conductivity below 60 MHz linked to the ionic movements.

Weighted nonlinear least squares optimization algorithm was implemented in Matlab (R2017a, The MathWorks, Inc., Natick, MA, US) to fit the parametric model to the experimental data over the specified frequency range.

III. RESULTS AND DISCUSSION

The post-processed values of the measurements performed on *ex vivo* ovine adrenal glands are reported in Fig. 2; the averaged values of the relative permittivity and effective conductivity of the two layers composing the adrenal gland are plotted with their variability. The experimental data of the two functional tissues composing the adrenal gland highlight a sizable difference in the dielectric properties between the two tissues: 15% in the relative permittivity and 17% in the effective conductivity averaged over the frequency band from 0.5 GHz to 8 GHz. The knowledge of the dielectric difference between cortex and medulla could be further exploited to optimize the EM based energy delivery in the tissue.

Fig. 3 shows the two pole Cole-Cole fit to the data of the functional tissues of *ex vivo* ovine adrenal glands from 0.5 GHz to 8 GHz; the average values across the different measurements for a given tissue type are plotted together with the Cole-Cole model. Table III shows the values of the Cole-Cole parameters calculated for each tissue type of the ovine models. For comparison, the Cole-Cole parameters for each functional tissue of *ex vivo* bovine adrenal glands reported in [28] are included. Fig. 3 illustrates the excellent fit of the two-pole Cole-Cole model to the *ex vivo* ovine data over the entire frequency range that was considered, with an accuracy better than 1%. In addition, the Cole-Cole parameters calculated in this study for *ex vivo* ovine adrenal tissues agree with the literature data reported in [28] regarding bovine adrenal glands. Quantitative differences are observed between the relative permittivity and the effective conductivity values obtained in this study and the values related to *ex vivo* bovine adrenal tissues; namely the relative permittivity of ovine adrenal medulla and cortex are approximately 5% lower than the values of *ex vivo* bovine tissues. Regarding the effective conductivity, the values of adrenal medulla and cortex are respectively 4% and 10% lower than the values of *ex vivo* bovine samples. Nonetheless, there are no relevant qualitative differences in the dispersion trends over the same frequency range. Typically, the quantitative differences in relative permittivity value can be attributed to variations in tissue temperature and/or environmental conditions or to the differences in water content between the two mammalian species. On the other hand,

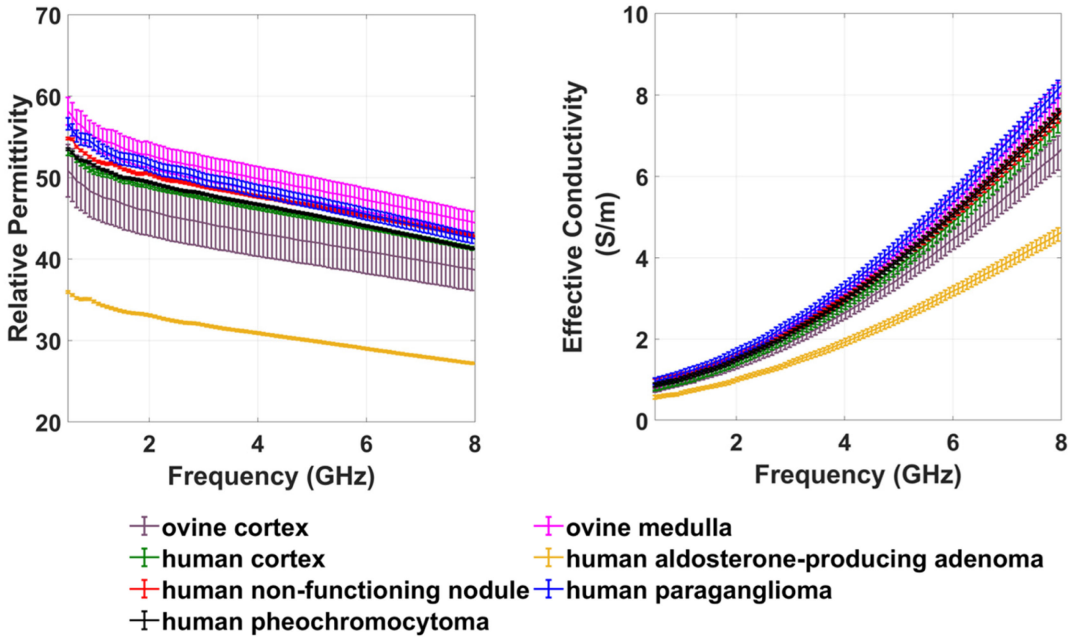

Fig. 2. Mean and standard deviation values of relative permittivity and effective conductivity reported for cortex and medulla of ex vivo ovine adrenal glands, normal tissue and diseased tissues (non-functioning nodule, paraganglioma, pheochromocytoma and aldosterone producing adenoma) of ex vivo human adrenal glands.

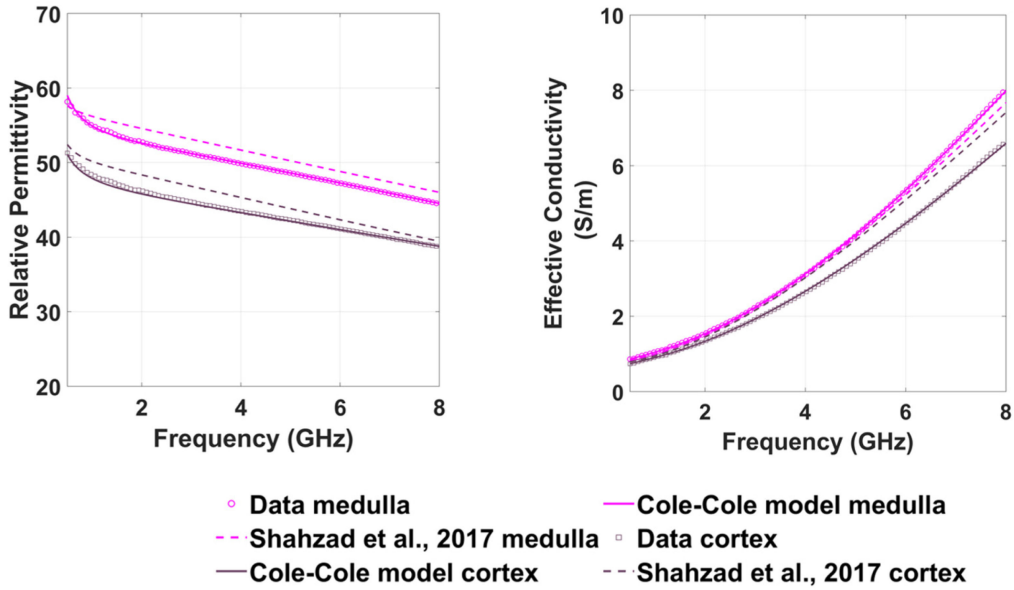

Fig. 3. Relative permittivity and effective conductivity of adrenal cortex and medulla in the frequency range 0.5-8 GHz: data and two pole Cole-Cole model from this study, and reference from literature [28].

an excellent match in the values of effective conductivity is visible between the two different species.

Together with the ovine data, Fig. 2 shows the values of relative permittivity and effective conductivity of diseased adrenal tissues excised from six different patients. The mean values of available dielectric properties of normal cortex tissue were also reported.

Comparable results between the normal *ex vivo* human adrenal cortex and the ovine adrenal cortex can be observed in Fig. 2. The average value of the cortical human tissue is approximately 6% higher than ovine adrenal cortex for both relative permittivity and effective conductivity over the frequency range.

Looking at the pheochromocytoma data (collected from 3 different samples), in comparison with the normal human adrenal cortex data, we can observe no substantial difference between the two groups of data; they differ less than 1% in relative permittivity and less 4% in effective conductivity values.

For paraganglioma, data were collected only from one sample and it appears noticeably more conductive than normal cortical tissue; relative permittivity and effective conductivity are 4% and 13% higher than normal human adrenal cortex over the frequency range.

Pheochromocytoma and paraganglioma arise from adrenal medulla and extra-adrenal paraganglia, respectively. Paraganglioma and pheochromocytoma are characterized by similar histological composition, and anatomical location is used as guideline to identify them [2], [3].

For non-functioning nodule, arising from the cortex, also data were collected only from one sample. When compared to normal human cortical tissue, the non-functioning nodule appears to differ less than 3% in relative permittivity and less than 6% in effective conductivity values.

According to the dielectric results reported in Fig. 2, only the dielectric values of the *ex vivo* human aldosterone-producing adenoma present sizable differences compared to the other diseased tissues. With respect to the normal *ex vivo* human dielectric values, aldosterone-producing adenoma is approximately 33% lower both in relative permittivity and effective conductivity values. The substantial differences in the dielectric values of the adrenocortical adenomas compared to the other types of diseases may be attributed to the characteristic abundant lipid composition of the aldosterone-producing adenomas. In addition, the infiltration of collagen fibres noticed through the histology analysis executed after the excision may further contribute to the lower dielectric values of the adreno-cortical adenoma. The other types of adrenal abnormalities, i.e. non-functioning nodule, paraganglioma and pheochromocytoma are not characterized by a lipidic composition.

This study provides new insights into the dielectric properties of adrenal glands of different animal species as well as normal and diseased human adrenal tissues. This study is the starting point for a more extensive dielectric characterization of the adrenal glands at temperatures of interest for MWA. Studies on dielectric properties as function of the temperature have been conducted only in liver so far; and have showed a correlation with the water content of the tissue (varying with the temperature increase) [17]–[20]. A decrease of about 20% in the water content and of 37-33% in the relative permittivity and effective conductivity of the liver when the temperatures overcome 60 °C was observed.

The design of this study did not allow us to access the inner part of the human adrenal gland, i.e. the medulla. Among the tumours investigated, the paraganglioma appears to show a sizable difference when compared with normal human cortex in terms of effective conductivity; and the conductive values observed are closer to the ovine medulla data reported. Therefore, further investigations on human samples should be conducted and designed to access such target. Moreover, further data should be collected to support the interesting preliminary data observed, especially the results concerning the aldosterone-producing adenomas, responsible for PA. The dielectric difference between the PA adenoma, and the surrounding cortex, may suggest the investigation of novel EM-based diagnostic imaging techniques [40]–[42] in the detection of such tumours.

IV. Conclusion

In this study the results of the dielectric characterization of *ex vivo* ovine adrenal models are reported. The tissue properties were investigated in the frequency range from 0.5 GHz to 8 GHz in order to include the main frequencies of interest for microwave thermal ablation (i.e. 915 MHz, 2.45 GHz and 5.8 GHz). In addition, the dielectric data of normal and diseased *ex vivo* human adrenal gland are presented. To the best of authors' knowledge, this is the first study where an accurate characterization of *ex vivo* ovine adrenal glands as well as dielectric data of normal and diseased *ex vivo* human adrenal glands were provided.

The results of this study indicate that no substantial differences exist in *ex vivo* adrenal functional tissues for different mammalian species. Moreover, the dielectric properties of normal *ex vivo* human adrenal tissues are in agreement with the values of the ovine models, confirming that ovine adrenal glands represent a feasible model to be adopted in pre-clinical numerical and experimental studies. Finally, this study showed that out of various adrenal gland diseases only aldosterone-producing adenomas show noticeably lower values in relative permittivity than the other types of diseases.

However, further measurements are required to confirm and support these preliminary data and better compare the dielectric properties of *ex vivo* animal and human adrenal glands. The accurate characterization of such properties is fundamental in the development and optimization of EM based therapeutic solutions such as the recently investigated MWA based selective treatment of shallow adenomas arising from the cortex of the adrenal gland and responsible for hypersecretion of aldosterone hormone and persistent hypertension.

References

[1] J. Hall *et al.*, *Guyton and Hall textbook of medical physiology*, 12th ed. Philadelphia, PA.: Saunders/Elsevier, 2010.
[2] A. K. Lam, "Update on adrenal tumours in 2017 World Health Organization (WHO) of endocrine tumours," *Endocr. Pathol.*, vol. 28, no. 3. pp. 213–227, 2017.
[3] H. P. H Neumann, "Pheochromocytoma and Paraganglioma," *N. Engl. J. Med.*, vol. 381, no. 6. pp. 552–565, 2019.
[4] W. F. Young, "Primary aldosteronism: Renaissance of a syndrome," *Clin. Endocrinol.*, vol. 66, no. 5. pp. 607–618, 2007.
[5] J. W. Funder, *Primary Aldosteronism: Present and Future*, 1st ed., vol. 109, Elsevier Inc., 2019.
[6] C. Catena *et al.*, "Mineralocorticoid antagonists treatment versus surgery in primary aldosteronism," *Horm. Metab. Res.* vol. 42, no. 6, pp. 440–445, 2010.
[7] P. Mulatero *et al.*, "Increased diagnosis of primary aldosteronism, including surgically correctable forms, in centers from five continents," *J. Clin. Endocrinol. Metab.*, vol. 89, no. 3, pp. 1045–1050, 2004.
[8] G. P. Rossi *et al.*, "Vascular remodeling and duration of hypertension predict outcome of adrenalectomy in primary aldosteronism patients," *Hyperthension*, vol. 51, no. 5, pp. 1366–1371, 2008.
[9] M. Ahmed, *et al.*, "Principles of and advances in percutaneus ablation," *Radiology*, vol. 258, no. 2, pp. 351–369, 2011.
[10] Chris Brace, "Thermal tumor ablation in clinical use," *IEEE Pulse*., vol. 2, no. 5, pp. 28–38, Sep.-Oct. 2011.
[11] H. Fallahi *et al.*, "Microwave antennas for thermal ablation of benign adrenal adenomas," *Biomed. Phys. Eng. Exp.*, vol. 5, no. 2, pp. 25–44, 2019.
[12] P. T. Donlon *et al.*, "Using microwave thermal ablation to develop a subtotal, cortical-sparing approach to the management of primary aldosteronism," *Int. J. Hyperther.*, vol. 36, no. 1, pp. 905–914, 2019.
[13] S. N. Goldberg *et al.*, "Thermal ablation therapy for focal malignancy," *Am. J. Roentgenol.*, vol. 174, no. 2, pp. 323–331, 2000.

[14] V. Lopresto *et al.*, "Treatment planning in microwave thermal ablation: clinical gaps and recent research advances," *Int. J. Hyperther.*, vol. 33, no. 1, pp. 83–100, 2017.
[15] J. F. Sawicki *et al.*, "The impact of frequency on the performance of microwave ablation," vol. 33, no. 1, pp. 61–68, 2017.
[16] F. Hojjatollah *et al.*, "Antenna designs for microwave tissue ablation," *Crit. Rev. Biomed. Eng.*, vol. 46, no. 6, pp. 495–521, 2019.
[17] V. Lopresto *et al.*, "Changes in the dielectric porperties of *ex vivo* bovine liver during microwave thermal ablation at 2.45 GHz," *Phys. Med. Biol.*, vol. 57, no. 8, pp. 2309–2327, 2012.
[18] Z. Ji *et al.*, "Expanded modeling of temperature-dependent dielectric properties for microwave thermal ablation," *Phys. Med. Biol.*, vol. 56, no. 16, pp. 5249–5264, 2011.
[19] G. Ruvio *et al.*, "Comparison of coaxial open-ended probe based dielectric measurements on ex-vivo thermally ablate tissue," in *Proc. 13th European Conf. Antennas Propag.*, 2019, pp. 1–4.
[20] H. Fallahi *et al.*, "Broadband dielectric properties of *ex vivo* bovine liver tissue characterized at ablative temperature," *IEEE Trans. Biomed. Eng.*, vol. 68, no. 1, pp. 90–98, Jan. 2021.
[21] A. P. O'Rourke *et al.*, "Dielectric properties of human normal, malignant and cirrhotic liver tissue: In vivo and *ex vivo* measurements from 0.5 to 20 GHz using a precision open-ended coaxial probe," *Phys. Med. Biol.*, vol. 52, no. 15, pp. 4707–4719, 2007.
[22] A. Martellosio *et al.*, "Dielectric properties characterization from 0.5 to 50 GHz of breast cancer tissues," *IEEE Trans. Microw. Theory Tech.*, vol. 65, no. 3, pp. 998–1011, Mar. 2017.
[23] M. Lazebnik *et al.*, "A large-scale study of the ultrawideband microwave dielectric properties of normal breast tissue obtained from reduction surgeries," *Phys. Med. Biol.*, vol. 52, no. 10, pp. 2637–2656, 2007.
[24] C. Gabriel *et al.*, "The dielectric properties of biological tissues : I. Literature survey survey," *Phys. Med. Biol.*, vol. 41, no. 11, pp. 2231–2249, 1996.
[25] B. Amin *et al.*, "Anthropomorphic calcaneus phantom for microwave bone imaging applications," *IEEE J. Electromagn.*, RF, Microw. Med. Biol., early access, 2020.
[26] X. Yu *et al.*, "Dielectric properties of normal and metastatic lymph nodes *ex vivo* from lung cancer surgeries," *Bioelectromagnetics*., vol. 41, no. 2, pp. 148–155, 2020.
[27] A. Peyman *et al.*, "Dielectric properties of porcine glands, gonads and body fluids," *Phys. Med. Biol.*, vol. 57, no. 19, pp. 339–344, 2012.
[28] A. Shahzad *et al.*, "Broadband dielectric properties of adrenal gland for accurate anatomical modelling in medical applications," in *Proc. Int. Conf. Electromagnetics Adv. Appl.*, Verona, Italy, 2017, pp. 1465–1468.
[29] G. Ruvio *et al.*, "Numerical evaluation of microwave thermal ablation to treat small adrenocortical masses," *Int. J. RF Microw. Comput. Eng.*, vol. 28, no. 3, pp. 1–8, 2018.
[30] A. Bottiglieri *et al.*, "Exploiting tissue dielectric properties to shape microwave thermal ablation zones," *Sensors*, vol. 20, no. 14, pp. 3960–3975, 2020.
[31] L. O. Lerman *et al.*, "Animal models of hypertension: A scientific statement from the American heart association," *Hypertension*, vol. 73, no. 6, pp. 87–120, 2019.
[32] P. C. Qian *et al.*, "Transvascular pacing of aorticorenal ganglia provides a testable procedural endpoint for renal artery denervation," *JACC. Cardiovasc. Interv.*, vol. 12, no. 12, pp. 1109–1120, 2019.
[33] D. H. Abbott *et al.*, "Nonhuman primates as models for human adrenal androgen production: Function and dysfunction," *Rev. Endocr. Metab. Disord.*, vol. 10, no. 1, pp. 33–42, 2009.
[34] P. M. Meaney *et al.*, "Open-ended coaxial dielectric probe effective penetration depth determination," *IEEE Trans. Microw. Theory Techn.*, vol. 64, no. 3, pp. 915–923, Mar. 2016.
[35] A. La Gioia *et al.*, "Quantification of the sensing radius of a coaxial probe for accurate interpretation of heterogeneous tissue dielectric data," *IEEE J-ERM*, vol. 2, no. 3, pp. 145–153, Sep. 2018.
[36] A. La Gioia *et al.*, "Open-ended coaxial probe technique for dielectric measurement of biological tissues: Challenges and common practices," *Diagnostics*, vol. 8, no. 2, pp. 1–38, 2018.
[37] A. Peyman *et al.*, "Complex permittivity of sodium chloride solutions at microwave frequencies," *Bioelectromagnetics*, vol. 28, no. 4, pp. 264–274, 2007.
[38] C. Gabriel *et al.*, "Dielectric measurement : error analysis and assessment of uncertainty," *Phys. Med. Biol.*, vol. 51, pp. 6033–6046, 2006.
[39] B. N. Taylor *et al.*, "Guidelines for evaluating and expressing the uncertainty of NIST measurement results," United States Dept. Commerce, Washington, DC, USA, NIST Tech. Note 1297, 1994.
[40] G. G. Bellizzi *et al.*, "A full-wave numerical assessment of microwave tomography for monitoring cancer ablation," in *Proc. 11th European Conf. Antennas Propag.*, 2017, pp. 3722–3725.
[41] A. Bottiglieri *et al.*, "Monitoring microwave thermal ablation using electrical impedance tomography: An experimental feasibility study," in *Proc. 14th European Conf. Antennas Propag.*, 2020, pp. 1–5.
[42] M. T. Bevacqua *et al.*, "Potentialities of inverse scattering techniques for breast cancer imaging at millimeter-waves frequencies," in *Proc. 14th European Conf. Antennas Propag.*, 2020, pp. 1–3.

Anna Bottiglieri received the bachelor's and master's degrees in biomedical engineering from the University of Rome-La Sapienza, Rome, Italy, with first-class of honors. She is currently working toward the Ph.D. degree with Translational Medical Device Lab, Galway, Ireland. During the master's degree she worked to enhance the performance of an UWB system used to detect breath and cardiac frequencies, noninvasively. She worked on projects in collaboration with the University of Wisconsin-Madison, Madison, WI, USA. Her current research interests in on the novel approaches for microwave thermal ablation and numerical modeling of critical targets. Her research interests include dielectric characterization and histology analysis of biological tissues. She is a member of the COST Action MyWave CA17115.

Atif Shahzad received the B.Sc. (Hons.) degree in computer engineering from COMSATS University, Lahore, Pakistan, in 2006, the M.Sc. degree in electronic engineering from the University of Leeds, Leeds, U.K., in 2009, and the Ph.D. degree in medical engineering from the National University of Ireland Galway, Galway, Ireland, in 2015. He is currently a Research Lecturer in medical technologies and the Co-Director with the Smart Sensors Lab, National University of Ireland, Galway, Ireland. His research interests include medical sensing technologies, device development, signal and image processing, and artificial intelligence in healthcare.

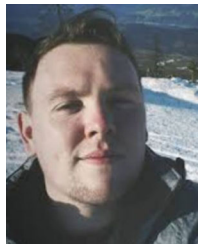

Padraig Donlon received the B.Sc. degree in genetics and cell biology from Dublin City University, Dublin, Ireland, and the master's degree (first-class Hons.) in regenerative medicine from the National University of Ireland Galway, Galway, Ireland. He is currently working toward the Ph.D. degree with the Adrenal Research Lab. He is currently working on the effects of hyperthermia on in vitro models of adrencortical tumors in the hope of discovering novel approaches for tumor treatment. He worked on projects in collaboration with Kansas State University, Manhattan, KS, USA.

Michael Conall Dennedy received the B.Sc. degree in pharmacology in 2000, the M.B., B.A.O., B.Ch. degree in 2002, the MD degree in obstetrics in 2007, and the Ph.D. degree in medicine in 2013. He is currently a Consultant Endocrinologist with Galway University Hospital, Galway, Ireland, and a Senior Lecturer in therapeutics with the National University of Ireland (NUI) Galway, Galway, Ireland. He trained through the HSE/HRB National SpR Academic Fellowship Programme, an integrated academic clinician scientist programme. Following this, he completed a fellowship in endocrinology with the University of Cambridge, Cambridge, U.K., and Addenbrooke's hospital. He assumed his current post in February 2014. His research interest focuses on the pathogenesis and treatment of functional adrenal tumors, both benign and malignant. He is a member of the European Network for the Study of Adrenal Tumour working Groups for adrenocortical carcinoma, aldosterone producing adenomas, phaeochromocytoma and non aldosterone producing adrenocortical adenomas. He retain links with the Institute of Metabolic Science, University of Cambridge, and has forged collaborations with Centre for Endocrinology, Diabetes and Metabolism, University of Birmingham, Birmingham, U.K. He is also affiliated with the CURAM programme, NUI, Galway and the Translational Medical Device Laboratory, Galway, Ireland.

Dr. Dennedy is the Director for the Welcome/HRB Irish Clinical Academic Training (ICAT) Programme and the corecepient of this award. He is also the Director of the undergraduate MB/Ph.D. programme with NUI, Galway. He is the Specialty Director of endocrinology with the Royal College of Physicians of Ireland's, International Clinical Fellows Programme.

Aoife Lowery received the master's degree in medical science from the National University of Ireland Galway, Galway, Ireland, and the Ph.D. degree as part of the Molecular Medicine Ireland Clinician Scientist Fellowship Programme. She is currently an Associate Professor with the Discipline of Surgery, National University of Ireland Galway, Galway, Ireland, and an Endocrine and Breast Surgeon with Galway University Hospital, Galway, Ireland. She completed her clinical and surgical training with the National University of Ireland Galway (M.B., B.Ch., B.A.O., M.R.C.S.) and the Royal College of Surgeons, Ireland Higher Surgical Training Programme (FRCS). Following her surgical training in Ireland, she also completed an International Fellowship in Endocrine Surgery with France's pre-eminent Endocrine Surgery unit in Marseille, funded by the Richard Steeven's Scholarship. Her research interests predominantly include endocrine disease and breast cancer with a translational science approach enhanced by her closely aligned clinical subspecialty interest in endocrine and breast surgery, and the investigation of innovative minimally invasive approaches to locoregional tumor control. Her ongoing work on these themes investigates factors that drive tumor intitation and locoregional disease recurrence and the implications that the molecular heterogeneity of malignancy may have on surgical strategy. Dr. Lowery is currently Year 5 Head for the Undergraduate Medical Education Programme, and is an Associate Director with ICAT. She was the recipient of both the Millen (RCSI Millen Lecturer 2015) and the Smith Medals (ASGBI Robert Smith Lecturer 2019).

Martin O'Halloran (Member, IEEE) is currently a Professor in Medical Electronics and Science Foundation Ireland (SFI) Investigator, National University of Ireland Galway, Galway, Ireland. Reflecting the interdisciplinary nature of his research, he holds a joint affiliation with the College of Engineering and Informatics and the College of Medicine, Nursing and Health Sciences, and leads the Translational Medical Device Laboratory, Lambe Institute. Dr. O'Halloran has received more than 30 national and international research awards, and was recently awarded SFI's Early-Stage Researcher of the Year, Engineers Ireland Chartered Engineer of the Year, and the European Research Council's Starting Investigator Grant. He was a Co-Proposer of a European COST Action (entitled "MiMED") and is now leading a network of more than 180 medical device researchers from 24 countries, focused on the clinical evaluation and commercialization of novel medical devices in Europe. Over the last six years, he has personally secured €10.6 million in direct research funding and has published more than 180 papers in peer-reviewed journals. He has been an Invited Chair and Invited Speaker with several major electromagnetics and translational medicine conferences/seminars. He is currently Non-executive Director of the BioInnovate programme, and Co-Lead of the Health Innovation Hub Ireland at NUI Galway.

Laura Farina (Member, IEEE) received the B.Sc. degree in clinical engineering in 2010, the M.Sc. degree in biomedical engineering in 2013 and the Ph.D. degree in information and communication technology –applied electromagnetism in 2017, from Sapienza University of Rome, Italy.

Her research activity has been focused on the experimental and numerical characterization of the electromagnetic, thermal and physical changes undergone by tissues treated with microwave ablation procedures. She worked also in projects involving nanoparticle manipulation, dielectric spectroscopy and microwave imaging in collaboration with different laboratories in academia and industry, in Italy, Israel, Czech Republic, Malta, and Ireland. Now, her research is focused on the development of novel microwave ablation systems for critical targets, with attention to the treatment of functional adrenal adenomas causing hypertension and lung cancer. She collaborates with start-ups and small companies developing novel electromagnetic thermal ablation devices. In the last 6 years, she secured 17 publications on peer-reviewed journals, and more than 30 conferences contributions.

Dr. Farina participated in two already completed COST Actions and she is Management Committee Substitute for Ireland for the current COST Action MyWave CA17115. She is member of the ASME Thermal Medicine Committee and former member of the Italian Society of electromagnetism. She is a Marie Skłodowska-Curie MedTrain Fellow with CÚRAM in the Translational Medical Device Lab at the National University of Ireland, Galway.